

Statistical properties of directed avalanches

N. Zh. Bunzarova*

*Bogoliubov Laboratory of Theoretical Physics, JINR, 141980 Dubna, Russia
and Institute of Mechanics, Bulgarian Academy of Sciences, 1113 Sofia, Bulgaria*

(Received 5 March 2010; revised manuscript received 28 May 2010; published 13 September 2010)

A two-dimensional directed stochastic sandpile model is studied both numerically and analytically. One of the known analytical approaches is extended by considering general stochastic toppling rules. The probability density distribution for the first-passage time of stochastic process described by a nonlinear Langevin equation with power-law dependence of the diffusion coefficient is obtained. Large-scale Monte Carlo simulations are performed with the aim to analyze statistical properties of the avalanches, such as the asymmetry between the initial and final stages, scaling of voids and the width of the thickest branch. Comparison with random walks description is drawn and different plausible scenarios for the avalanche evolution and the scaling exponents are suggested.

DOI: [10.1103/PhysRevE.82.031116](https://doi.org/10.1103/PhysRevE.82.031116)

PACS number(s): 05.40.-a, 05.65.+b, 02.50.Ey, 82.20.-w

I. INTRODUCTION

Sandpile models of self-organized criticality (SOC) have received considerable interest as the simplest models describing avalanchelike dynamics, observed in many systems in nature. In 1987 Bak, Tang and Wiesenfeld (BTW) [1] proposed a simple cellular automaton model of sandpile evolution, which is deterministic and isotropic. The BTW model became a paradigmatic model for studies of SOC but, despite its rather simple definition and the great interest, there is still no rigorous derivation of the full set of critical exponents in two dimensions.

Starting with the first analytical attempts to derive the scaling exponents of the isotropic sandpile model with deterministic toppling rules, the following program was usually performed [2,3]. One starts with coarse graining of the microscopic particle dynamics, keeping the main underlying symmetries. This gives rise to nonlinear stochastic differential equations containing a diffusion term and noise term(s). The nonlinearity comes from the step function which describes the threshold condition for avalanche initiation. As a rule, a simple nonlinear term is left to mimic the discrete step function. The noise terms are of two kinds: an internal, conservative noise, which accounts for the integrated out microscopic degrees of freedom; the external, nonconservative noise turns out to be the relevant one for the dynamics of the system. The resulting equations can be analyzed by means of the dynamic renormalization group to extract values of the critical exponents [2,3].

The establishment of the Abelian properties of the model [4] enhanced its analytical tractability and some important characteristics of the stationary state have been obtained exactly, see, e.g., [5–7].

Another essential simplification arises from the introduction of directed toppling rules, which makes models mathematically simpler. Indeed, in 1989 Dhar and Ramaswamy [8] introduced and solved exactly in all dimensions a directed version of the BTW sandpile model. Later, Manna [9]

presented the first sandpile with stochastic toppling rules. The model is isotropic, with multiple toppling of sites within an avalanche. Notably, the presence of stochastic elements does not alter the Abelian structure of the model.

A lot of work was done to compare analytically and numerically deterministic and stochastic directed sandpiles with the aim to define their universality classes. The existence of multiple topplings seems to be the main difficulty for obtaining exact solutions, even for directed stochastic sandpiles, which explains why there are very few analytical works on these models. The early theoretical works suggest that the original deterministic BTW sandpile and the stochastic Manna sandpile belong to the same universality class [10–12]. However, further computer simulations of directed sandpile models have shown that the deterministic and stochastic models belong to two different universality classes, in agreement with the analytical results obtained by Paczusky and Bassler [13] and by Kloster, Maslov, and Tang [14].

Here we confine ourselves to the discussion of two-dimensional directed sandpiles with stochastic toppling rules and boundary dissipation. The reader interested in the identification of the universality classes for one-dimensional directed models is referred to [15] and references therein. The aim of our investigations is to study in more detail the morphology of large directed avalanches and its effect on their statistical properties during the entire evolution. To this end we introduce an approach—evaluation of basic characteristics over ensembles of avalanches with (almost) fixed time duration, less than the lattice size in the temporal direction. This approach opens the perspective of defining new sets of scaling laws for the final stage of the avalanche evolution. We hope also our results to shed light on the possibility of alternative values of the scaling exponents.

In Sec. II we fix the notation by defining the scaling laws usually used to describe the statistical properties of directed avalanches. Here we also give a short overview of the contemporary estimates of the scaling exponents by means of Monte Carlo simulations. The two analytic theories [13,14], which predict exponents in agreement with the numerical results, are reviewed in the first two subsections of Sec. III. Then in Sec. III C, we report an extension of the existing

*nadezhda@imbm.bas.bg

theory to directed sandpiles with stochastic toppling rules which allow, with arbitrary probability, toppling of one particle, as well as toppling of two particles at a time. The approach of [14] is generalized with the derivation of a Langevin equation in this case. We prove that, as expected, the above generalization of the toppling dynamics changes only the numerical coefficient in front of the position-dependent diffusion constant and does not alter the universality class of the model. Next, the fundamental solution of the Fokker-Planck equation, corresponding to power-law dependence with exponent $0 \leq \gamma < 1$ of the diffusion coefficient, is found. By using conventional methods, we have obtained there from an explicit expression for the probability density of the first-passage time distribution and, in particular, its power-law exponent $\tau_t = (3 - 2\gamma)/(2 - 2\gamma)$. In Sec. IV A we comment on the validity of the random walk description of basic statistical parameters of directed avalanches. It is shown that the conditional time-dependent average values of the avalanche front width and number of unstable sites, averaged over avalanches of almost fixed length, can be characterized by power-law exponents at the terminal point, different from the exponents at the initial point. A number of original results of computer simulations, which contradict the simple random walk picture, are presented too. A finite-size scaling analysis of avalanche characteristics in restricted ensembles of avalanches with duration in intervals of the form $[T, 1.017T]$, where $T = 1000, 2000, 4000,$ and 8000 , is given in Sec. IV B. Here we present also data on the finite-size effects on the different scaling exponents. Section V contains a critical discussion of the existing theories and some alternatives allowing for values of the critical exponents different from the established ones. The paper closes with a summary of the main results.

II. DESCRIPTION OF DIRECTED AVALANCHES. OVERVIEW OF MONTE CARLO RESULTS

Two-dimensional directed sandpile models are usually defined on a square lattice of linear size L , either with the standard orientation, or rotated by the angle of $\pi/4$. To each site of the lattice an integer variable z_i , measuring the number of sand grains (height) or energy quanta, is assigned. Grains are added to randomly chosen sites, thus increasing their height by one, $z_i \rightarrow z_i + 1$. When the height at a given site becomes larger than or equal to a threshold value z_c , that site topples. The case of standard orientation has been considered, e.g., by Vazquez [16] and by Pastor-Satorras and A. Vespignani [17]. Topplings are directed along a fixed principle axis x_{\parallel} of the lattice, defined usually as “downward” and considered as virtual time axis. In the case of deterministic rules, $z_c = 3$ and when a site in a row x_{\parallel} topples, it sends three grains to the nearest neighbor and each of the two next-nearest neighbor sites in the next row $x_{\parallel} + 1$. In the stochastic version, $z_c = 2$ and two grains are sent to two sites randomly chosen among the above three neighbors in the row $x_{\parallel} + 1$. The toppling rules of this model are defined as exclusive if the two energy grains are always distributed on different sites (ESDS) and nonexclusive (NESDS) if the dynamics rules allow the transfer of two energy grains onto the

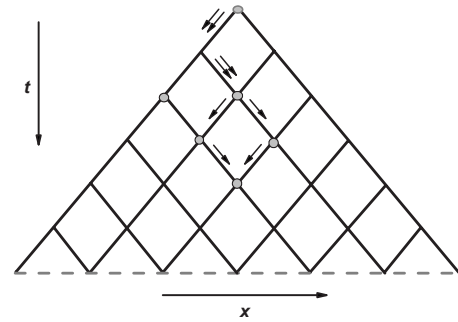


FIG. 1. Schematic representation of the rotated by $\pi/4$ square lattice and the directed toppling rules. The bottom boundary of the lattice is open. In previous works only two particles were allowed to topple.

same site. The boundary conditions are periodic in the transverse direction x_{\perp} and open at $x_{\parallel} = L$ (boundary dissipation). The dynamics is locally conservative since no energy grains are lost during the toppling events.

Alternatively, Alcaraz and Rittenberg [18] considered directed stochastic sandpiles defined on the rotated by $\pi/4$ square lattice, see Fig. 1 for example. The direction of propagation is down the diagonal of the squares, and the bottom boundary is open. The grains are added always at the top site. The avalanche threshold is $z_c = 2$ and when a site topples, the following four events can take place with different probabilities: two particles are transferred to the (a) left or (b) right nearest neighbor in the downstream layer, only one particle is transferred to the (c) left or (d) right nearest neighbor in the next layer.

Directed avalanches are characterized by the total number of toppled particles s (called “size”), the time duration t (called “length”) and transversal extent x (called “width”). According to finite-size scaling (FSS), the asymptotic form of the corresponding probability distribution densities is given by

$$p_s(s) \approx s^{-\tau_s} g(s/s_c), \quad (1)$$

$$p_t(t) \approx t^{-\tau_t} f(t/t_c), \quad (2)$$

$$p_x(x) \approx x^{-\tau_x} w(x/x_c), \quad (3)$$

where the exponents τ_s , τ_t , and τ_x characterize the critical behavior and define the universality classes to which the models belong; s_c , t_c , and x_c are finite-size cutoff parameters. In the thermodynamic limit ($L \rightarrow \infty$), the characteristic avalanche size, length and width diverge as $s_c \sim L^D$, $t_c \sim L^z$, and $x_c \sim L^{1/\zeta}$, respectively, where D defines the fractal dimension of the avalanche cluster, z and ζ are dynamical critical exponent ($z = 1$ for directed sandpiles). The average avalanche size corresponds to the number of topplings needed for a grain to reach the boundary; i.e., $\langle s \rangle \sim L$. On the other hand, by using expression (1) for the density of the size probability distribution, one obtains

$$\langle s \rangle \simeq \int_1^\infty s^{1-\tau_s} g(sL^{-D}) ds \sim L^{D(2-\tau_s)}. \quad (4)$$

Hence, the relationship $D=1/(2-\tau_s)$ follows, which indicates that not all of the above exponents are independent. Indeed, conservation of probability, i.e., equality of the integrated right-hand sides of the scaling Eqs. (1)–(3), yields: $\tau_t-1=D(\tau_s-1)=(\tau_x-1)/\zeta$ [13]; the first of these equalities in combination with $(2-\tau_s)D=1$ implies the result $\tau_t=D$.

Numerical simulations of directed models with different toppling rules on two-dimensional lattices of size ranging from $L=64$ to $L=2048$ were done by Vazquez [16]. The results for the scaling exponents, obtained by the moment analysis technique after averaging over 10^8 avalanches, showed that the Manna and random-threshold directed models share the same universality class.

Large-scale Monte Carlo simulations of directed sandpile models with stochastic toppling rules have been reported by Pastor-Satorras and Vespignani in [17]. It was found that the stochastic and deterministic models belong to different universality classes. In the two-dimensional case with boundary dissipation, their estimates of the critical exponents for two types of dynamics, with exclusive (ESDS) and not exclusive (NESDS) toppling rules, are [17]

$$\text{ESDS: } \tau_s = 1.43(1), \quad D = 1.74(1),$$

$$\tau_t = 1.71(3), \quad z = 0.99(1),$$

$$\text{NESDS: } \tau_s = 1.43(1), \quad D = 1.75(1), \quad \tau_t = 1.74(4),$$

$$z = 0.99(1).$$

These results show that the ESDS and NESDS models are in the same universality class of the stochastic directed sandpiles (SDS). The results for deterministic directed sandpiles (DDS) are in agreement with the exact solution by Dhar and Ramaswamy [8] and show that the DDS and SDS models belong to different universality classes. The critical behavior was shown to be the same in the cases of bulk and boundary dissipation. The computer simulations were done for lattice sizes ranging from $L=100$ to $L=6400$ and statistical distributions were obtained by averaging over 10^7 avalanches. The spatial structure of the avalanches for both the DDS and SDS models was studied with the aim to understand the difference in their critical behavior. It seems that the difference can be explained by the presence of multiple toppling in SDS. In particular, the fractal dimension of the avalanche cluster is higher for the stochastic models ($D=7/4$) than for the deterministic ones ($D=3/2$).

The most recent Monte Carlo simulations have been done by Alcaraz and Rittenberg [18] on the rotated by $\pi/4$ square lattice, see Fig. 1. Their results, estimated for samples of up to 1.2×10^8 avalanches of sizes up to 30 000, show that the two-dimensional directed stochastic model belongs to a universality class with $\sigma_\tau = 1.780 \pm 0.005$. If the estimated error bars are correct, then this result is in contradiction with the analytical predictions [13,14], as well as with the previous numerical estimates [17].

We have also performed numerical simulations of a directed sandpile model on the lattice shown in Fig. 1. Our stochastic dynamics allows for the toppling of one or two particles with equal probabilities. The probability distributions for different parameters of the avalanches were studied, with a special focus on the spatial structure of finite-size avalanches and the statistical asymmetry between the initial and final stages of their evolution. Some of our new numerical results are presented in Secs. IV A, IV B, and V.

III. ANALYTIC APPROACHES

First we review two of the more recent analytical works which predict values of the scaling exponents in full agreement with the results of computer simulations reported in [17]. In [13] a continuous Langevin equation for the propagation of avalanches was derived and, on its basis, the exponents characterizing avalanches were calculated. In [14] an approach based on the analysis of the change in the total number of topplings from layer to layer was developed. The central result of this work is a stochastic equation which describes an unbiased random walk with a variable step size, proportional to the cubic root of the current position of the random walker. With the aid of some assumptions on the avalanche structure, an analytical derivation of the fractal dimension D of the unstable avalanche cluster and the exponent τ_t of the avalanche length distributions was given.

Next, we extend the theory in [14] by deriving a Langevin equation for more general toppling rules and relaxing the conjecture for diffusionlike growth with time of the number of unstable sites in the avalanche. Finally, we solve the Fokker-Planck equation for a continuous random walk with fractional power-law dependence of the diffusion coefficient and derive an explicit expression for the first-passage time distribution.

A. Theory of Paczusky and Bassler

It should be noted that the multiple topplings in Abelian directed stochastic sandpiles have a different origin than those in the undirected BTW model. In the latter case they appear because of the wave nature of the avalanches [5]. In the Abelian models belonging to the SDS universality class multiple topplings occur due to the accumulation of many particles at an unstable site. Then, such a site can relax by a succession of topplings of particles in pairs or one-by-one. Alternatively, one may consider toppling of the number of excessive particles at once, provided the probability of the composite event is taken into account. Anyway, the possible collection of many particles at a site makes the unstable avalanche cluster three-dimensional, which is a serious complication of the problem.

One of the few analytical studies of Abelian directed stochastic sandpiles is devoted to a directed version of the Manna model introduced by Paczusky and Bassler [13]. They consider a rotated by $\pi/4$ square lattice with periodic boundary conditions in the transverse direction. The coordinate in the direction of propagation is denoted by t , where $0 \leq t \leq T$. To each site (x, t) of the lattice an integer variable

$z(x, t)$ is assigned. The grains are added to a randomly chosen site x_i on the top row $t=0$, so that $z(x_i, 0) \rightarrow z(x_i, 0)+1$. When the height $z(x, t)$ at a site (x, t) becomes larger than the critical value $z_c=1$, the site topples, $z(x, t) \rightarrow z(x, t)-2$, and with probability $1/4$ the two particles go to the same left or right nearest neighbor in the layer $t+1$, or with probability $1/2$ each of the two nearest neighbors $z(x-1, t+1)$ and $z(x+1, t+1)$ receives exactly one particle. In the case of boundary dissipation, no grains are lost during the toppling events, except at the open boundary $t=T$.

In [13] it was shown that the critical state of the above described SDS is a product measure state with average density $\rho=1/2$. The critical dynamics is described as a kind of generalized branching process propagating in an uncorrelated random medium. Since the number of grains that leave any unstable site is always even, sites which receive an even number of grains do not change the flux of particles. On the other hand, sites that receive an odd number of grains increase or decrease the flux by one unit, depending on whether they were occupied or empty in the initial stable configuration. The process is critical and the increase or decrease occurs with equal probability. Moreover, on the average each site will receive $1/2$ of the grains going into its upstream nearest neighbors. The random deviations from the mean values are considered to arise from two kinds of noise in the evolution equation for the number of grains $n(x, t)$ added to site (x, t) . Thus, the presence or absence of a grain at a given site (x, t) is a source of nonconservative noise. Since the flux may change by one unit only, the nonconservative noise $\eta(x \pm 1, t)$ enters into the evolution equation with a unit step function θ_o as a prefactor (called threshold function). The other source of noise is due to the random (binomial) distribution of the grains outgoing from a toppling site to its downstream nearest neighbors—that is a conservative noise described by a stochastic current $j(x \pm 1, t)$. The first two moments of the stochastic current follow directly from the binomial distribution. By expanding to leading order in gradients and time derivatives in the discrete evolution equation, the following stochastic differential equation was derived,

$$\frac{\partial n(x, t)}{\partial t} = \frac{1}{2} \nabla^2 n(x, t) - 2 \frac{\partial j(x, t)}{\partial x} + 2 \theta[n(x, t)] \eta(x, t). \quad (5)$$

Here, by the central limit theorem, the noise terms $j(x, t)$ and $\eta(x, t)$ are both Gaussian with zero mean values and second moments given by

$$\begin{aligned} \langle \eta(x, t) \eta(x', t') \rangle &= \frac{1}{2} \delta(x - x') \delta(t - t'), \\ \langle j(x, t) j(x', t') \rangle &= n(x, t) \delta(x - x') \delta(t - t'). \end{aligned} \quad (6)$$

By using dimensional analysis, the authors of [13] conclude that the conservative noise is irrelevant and ignore the second term in the right-hand side of Eq. (5). Next, they argue that since in the region covered by the avalanche $n(x, t) > 0$ then $\theta(n(x, t)) \equiv 1$ and their final result is the description of the avalanche dynamics by the linear Edwards-Wilkinson (EW) equation [19].

$$\frac{\partial n(x, t)}{\partial t} = \frac{1}{2} \nabla^2 n(x, t) + 2 \eta(x, t) \quad (7)$$

with the initial condition $n(x, 0) = \delta(x)$.

From dimensional analysis the authors derive $x_c \sim t_c^{1/2}$. Next, they assume that the maximum number of topplings, n_c , scales with the transverse extent of the avalanche as the roughness of the one-dimensional interface in the EW theory scales with the system size, i.e., $n_c \sim x_c^{1/2} \sim t_c^{1/4}$. Hence, the characteristic area a and size s of the avalanches obey the scaling laws $a \sim x_c t_c \sim t_c^{3/2}$ and $s \sim n_c x_c t_c \sim t_c^{7/4}$ [13]. Because all the geometric characteristics associated with avalanches exhibit scaling behavior, it was assumed that the distributions of avalanche sizes, time durations and transversal spatial extent obey the power scaling laws [Eqs. (1)–(3)]. Since $D=7/4$, from the relations between the scaling exponents it follows that $\tau_s=10/7$, $\tau_t=7/4$, and $\tau_x=5/2$.

B. Theory of Kloster, Maslov, and Tang

Kloster, Maslov, and Tang [14] proposed a similar to [13] study of the SDS model on the same lattice and, by using different analytical tools, obtained the same set of exponents. The model is defined on the same rotated square lattice with periodic boundary conditions in the transversal direction $x_\perp = x_1 - x_2$ and open boundary conditions along the diagonal coordinate $x_\parallel = x_1 + x_2$. The sand is added to a randomly chosen site on the top row with $x_\parallel=0$ and falls off at $x_\parallel=L_\parallel$. The stochastic toppling rules are the same as in [13], see the previous subsection.

The total number of topplings in the layer x_\parallel is denoted by $N(x_\parallel) = \sum_{x_\perp} n(x_\perp, x_\parallel)$, where $n(x_\perp, x_\parallel)$ is the number of topplings of site (x_\perp, x_\parallel) . Hence, the number of grains passed from layer x_\parallel to the next layer $x_\parallel+1$ is $2N(x_\parallel)$. A site which gets an even number $2k$ of grains from a previous layer will always topple exactly k times, and will transfer the same $2k$ grains of sand to the next layer. Such sites, which do not change the total number of topplings $N(x_\parallel)$ from layer to layer, are called passive sites. On the other hand, any site which receives an odd number $2k+1$ of grains from the previous layer has the same chance to topple k times (if $z=0$ before the transfer) or $k+1$ times (if it had $z=1$). Such sites lead to decrease or increase by one of the total number of topplings and are called active sites. The main equation of [14] relates the change in the total number of topplings from layer $x_\parallel-1$ to layer x_\parallel to the number of active sites in the latter layer,

$$N(x_\parallel) = N(x_\parallel - 1) + \frac{1}{2} \sum_{a=1}^{N_a(x_\parallel)} \xi_a,$$

where all the random variables ξ_a take values -1 or $+1$ with equal probability and independently of each other. The two realizations of the random number ξ_a correspond to whether the active site labeled by a had $z=0$ or $z=1$ before the avalanche has reached it. Written in the continuum limit the main equation becomes

$$\frac{\partial N(x_{\parallel})}{\partial(x_{\parallel})} = \frac{1}{2} \sqrt{N_a(x_{\parallel})} \eta(x_{\parallel}), \quad (8)$$

where $\eta(x_{\parallel})$ is a normally distributed random variable with zero mean and unit variance. Equation (8) describes an unbiased random walk $N(x_{\parallel})$ with a variable step $\frac{1}{2}\sqrt{N_a(x_{\parallel})}$. By assuming $N(x_{\parallel}) \sim x_{\parallel}^{\alpha}$ and $N_a(x_{\parallel}) \sim x_{\parallel}^{\alpha_a}$, one obtains $N_a(x_{\parallel}) \sim N(x_{\parallel})^{\alpha_a/\alpha}$, and the solution of Eq. (8) yields $\alpha = (1 + \alpha_a)/2$ and $\tau_i = 1 + \alpha$, where τ_i is the exponent of the density of the probability distribution for the avalanche length, $p_i(x_{\parallel}) \sim x_{\parallel}^{-\tau_i}$. From the definition of the avalanche size $s = \sum_{i=1}^{x_{\parallel}} N(i) \sim x_{\parallel}^{1+\alpha} \sim x_{\parallel}^D$, the exponent relation $\tau_i = D$ for general directed sandpiles follows.

Next, to evaluate the exponent α_a , the authors of [14] note that because the grains are distributed independently, any site which has at least one toppled neighbor in the previous layer is equally likely to receive an even or odd number of particles, and the probability to become active site is 1/2. The exponent α_a defines how the number of distinct sites that topple at least once, scales with the layer number x_{\parallel} . Arguments, based on the assumption that for sufficiently large x_{\parallel} the number of active sites is proportional to the number of toppled sites, $N_a(x_{\parallel}) \sim N(x_{\parallel})$, and that the topplings in the layer x_{\parallel} are spread over the transversal direction according to the diffusion equation, $N(x_{\parallel}) \sim x_{\parallel}^{1/2}$, lead to the value $\alpha_a = 1/2$, hence $\alpha = 3/4$ and $\tau_i = D = 7/4$. The exponent for the avalanche size distribution is then $\tau_s = 1 + (\tau_i - 1)/D = 10/7$. Notably, since $\alpha_a/(2\alpha) = 1/3$, the step of the random walk described by Eq. (8) varies as a cubic root of the position.

As explained in [14], the difference between α and α_a comes from the presence of multiple toppling and $\alpha - \alpha_a$ determines how the average number of topplings $n_{top}(x_{\parallel})$ at a given site in the x_{\parallel} th layer scales with x_{\parallel} : $n_{top} \sim N/(2N_a) \sim x_{\parallel}^{\alpha - \alpha_a} = x_{\parallel}^{1/4}$.

An important feature of the stochastic directed models is that the set of toppled sites can have holes (inclusions of stable sites). In [14] it is supposed that these holes would mostly be concentrated near the boundaries of the avalanche in any given layer, while the core of the avalanche will be relatively holes free. As mentioned above, a site at a layer x_{\parallel} would typically topple $n_{top}(x_{\parallel}) \sim x_{\parallel}^{1/4}$ times within one avalanche. Since any of the $2n_{top}$ grains can go to each of the two nearest neighbors independent of others, for large n_{top} the situation where one of the neighbors would receive less than two grains and remain stable is exponentially unlikely. It is concluded that the creation of a new hole is exponentially suppressed. Therefore, for sufficiently large x_{\parallel} the number of active sites which is proportional to the number of toppled sites, should scale as $N_a \sim x_{\parallel}^{1/2}$.

The authors of [14] have presented also results of their own numerical simulations on lattices up to $x_{\parallel} \sim 100\,000$. The estimate of the exponent α agrees well with the analytical prediction, while the value of α_a is less clear. The locally determined exponent is appreciably higher than 1/2 in the region between $x_{\parallel} \sim 100$ and $x_{\parallel} \sim 10\,000$, reaching there the value of 0.6, but then goes down to the theoretical result $\alpha = 1/2$ in the end of the simulation range ($x_{\parallel} \sim 100\,000$).

The above analytical results are in good agreement with the simulation results of Pastor-Satorras and Vespignani [17],

as well as with the results of our own Monte Carlo simulations.

C. Derivation of a general Langevin equation

It is important to establish whether the results obtained in [13,14] are robust with respect to changes in the toppling rules. Here we consider the more general stochastic dynamics which allows an unstable site to send one particle to the next layer with probability μ_1 and two particles with probability $\mu_2 = 1 - \mu_1$. In the first case the particle goes to the left or to the right nearest neighbor with equal probability $\mu_1/2$, and in the second case with equal probability $\mu_2/3$ the two particles go to the right or to the left nearest neighbor, or each of the two nearest neighbors receives just one particle. Obviously, the toppling rules in [14] correspond to $\mu_1 = 0$, $\mu_2 = 1$. Here we shall develop the analytical theory for arbitrary values of the probabilities μ_1 , μ_2 . In the computer simulations we have chosen $\mu_1 = \mu_2 = 1/2$.

Following [14], we define *active sites* and *passive sites* depending on whether becoming unstable they do decrease/increase the particle flow to the next layer (active sites) or do not (passive sites). Let us now consider the probability for a given unstable site to remain with 0 or 1 particles after toppling. If the site has an even number $2k$, $k \geq 1$, of particles, then

$$\begin{aligned} P(2k \rightarrow 0) &= \sum_{p=0}^{k-1} \binom{2k-p-2}{p} \mu_1^{2(k-p)-2} \mu_2^{p+1} \\ &= \frac{\mu_2}{1 + \mu_2} (1 + \mu_2^{2k-1}), \\ P(2k \rightarrow 1) &= \sum_{p=0}^{k-1} \binom{2k-p-1}{p} \mu_1^{2(k-p)-1} \mu_2^p \\ &= \frac{1}{1 + \mu_2} (1 - \mu_2^{2k}). \end{aligned} \quad (9)$$

If the site has an odd number $2k+1$, $k \geq 1$, of particles, then:

$$\begin{aligned} P(2k+1 \rightarrow 0) &= \sum_{p=0}^{k-1} \binom{2k-p-1}{p} \mu_1^{2(k-p)-1} \mu_2^{(p+1)} \\ &= \frac{\mu_2}{1 + \mu_2} (1 - \mu_2^{2k}), \end{aligned}$$

$$P(2k+1 \rightarrow 1) = \sum_{p=0}^k \binom{2k-p}{p} \mu_1^{2(k-p)} \mu_2^p = \frac{1}{1 + \mu_2} (1 + \mu_2^{2k+1}). \quad (10)$$

Obviously, if $0 < \mu_2 < 1$ and if the avalanche dynamics is dominated by unstable sites with multiple topplings ($k \gg 1$), then the probability for a site with height $n \gg 1$ to become empty is approximately $P(n \rightarrow 0) \approx \mu_2/(1 + \mu_2)$, while the probability of remaining with one particle is approximately $P(n \rightarrow 1) \approx 1/(1 + \mu_2)$, independently of the (large) number n of particles before toppling. On the other hand the stationary

density of particles is $\rho_c(\mu_2)=1/(1+\mu_2)$ for any directed sandpile on acyclic graph [18]. Consequently, a given site is empty with probability $\mu_2/(1+\mu_2)$ and occupied with probability $1/(1+\mu_2)$. Now we recall that a passive site is a site which has been empty (occupied) in the stationary state and, after becoming unstable, has toppled to the same empty (occupied) stable state. Therefore, any unstable site at the avalanche front is passive with probability

$$P_0(\mu_2) = [1 - \rho_c(\mu_2)]P(n \rightarrow 0) + \rho_c(\mu_2)P(n \rightarrow 1) = \frac{1 + \mu_2^2}{(1 + \mu_2)^2}. \quad (11)$$

Similarly, any unstable site is active and increases the particle current by one with probability

$$P_+(\mu_2) = \rho_c(\mu_2)P(n \rightarrow 0) = \frac{\mu_2}{(1 + \mu_2)^2}, \quad (12)$$

which equals the probability of any unstable site to be active and decrease the particle current by one

$$P_-(\mu_2) = [1 - \rho_c(\mu_2)]P(n \rightarrow 1) = \frac{\mu_2}{(1 + \mu_2)^2}. \quad (13)$$

Expressions (11)–(13) hold true with exponential accuracy, terms of the order μ_2^n being neglected when $\mu_2 < 1$ and the occupation number $n \rightarrow \infty$. It should be noted that expressions of the same form have been derived in [18], see Eq. (41) there, for a one-dimensional stochastic directed model, by using an algebraic approach and asymptotic solution of recurrence relations.

Let $U(t)$ denote the set of unstable sites in the front of the avalanche at time $t=x_{||}$. Then the number of particles $N_p(t)$ transferred from layer t to layer $t+1$ satisfies the equation

$$N_p(t) = N_p(t-1) + \sum_{i \in U(t)} \zeta_i. \quad (14)$$

Here ζ_i are $N_u(t)=|U(t)|$ identically distributed random variables which take the values $-1,0,1$ with probabilities $P_-(\mu_2), P_0(\mu_2), P_+(\mu_2)$, respectively.

Assuming that $\zeta_i, i=1,2,\dots,N_u(t)$, are independent, and that asymptotically $N_u(t) \rightarrow \infty$, by the central limit theorem we obtain the convergence in distribution

$$\frac{1}{\sigma\sqrt{N_u(t)}} \sum_{i=1}^{N_u(t)} \zeta_i \rightarrow \mathcal{N}(0,1),$$

where $\sigma^2=2\mu_2/(1+\mu_2)^2$ is the variance of ζ_i , and $\mathcal{N}(0,1)$ is the normal distribution with zero expectation value and unit variance. Under the above assumptions the continuum-time limit in Eq. (14) yields the stochastic equation,

$$\frac{dN_p(t)}{dt} = \frac{\sqrt{2\mu_2}}{1 + \mu_2} \sqrt{N_u(t)} \eta(t), \quad (15)$$

where $\eta(t)$ is a $\mathcal{N}(0,1)$ distributed random variable.

The stochastic equation derived in [14] is a special case of our Eq. (15) which corresponds to stochastic dynamics with even number of topplings only, i.e., with $\mu_1=0, \mu_2=1$. Then, from Eqs. (9) and (10) one obtains,

$$P(2k \rightarrow 0) = P(2k+1 \rightarrow 1) = 1,$$

$$P(2k \rightarrow 1) = P(2k+1 \rightarrow 0) = 0.$$

In this case the stationary density of particles is $\rho_c(1)=\frac{1}{2}$. Active sites $N_a(t)$ are only those sites, which become unstable upon receiving an odd number of particles—on the average one half of the unstable sites at time t , $N_a(t) = \frac{1}{2}N_u(t)$. If a site was occupied (empty) in the stable configuration and at time t receives $2k+1$ particles, then it certainly increases (decreases) the flux of particles by one unit, due to $P(2k+2 \rightarrow 0)=1 [P(2k+1 \rightarrow 1)=1]$. These events occur with equal probability $P_+(1)=P_-(1)=\frac{1}{4}$, as follows from Eqs. (12) and (13) at $\mu_2=1$. Finally, an unstable site is passive with probability $P_0(1)=\frac{1}{2}$, see Eq. (11) at $\mu_2=1$. The stochastic equation derived in [14] follows from our Eq. (15) upon the substitution $N_p(t)=2N(t), N_u(t)=2N_a(t)$ and $\mu_2=1$,

$$\frac{dN(t)}{dt} = \frac{1}{2} \sqrt{N_a(t)} \eta(t). \quad (16)$$

In order to complete the theory one needs two kinds of additional conjectures, A and B. The first one (A) has to relate the number of unstable sites $N_u(t)$ to the number of transferred particles $N_p(t)$ in the growth phase of the avalanche. The second one (B) should assess the asymmetry between the growth and decay stages of the avalanche evolution and its effect on the overall exponents for finite-size avalanches.

General formulations of conjecture A follow from the definition of the fractal dimension of the avalanche cluster

$$\sum_{t'=1}^t N_p(t') \sim t^D \Rightarrow N_p(t) \sim t^{D-1}, \quad (17)$$

and the assumption $N_u(t) \sim t^\omega$, where, in the stage of avalanche growth, $D > 1$ and $\omega > 0$. Hence, one obtains $N_u(t) \sim [N_p(t)]^{\omega/(D-1)}$ and Eq. (15) becomes

$$\frac{dN_p(t)}{dt} = \frac{\sqrt{2\mu_2}}{1 + \mu_2} [N_p(t)]^{\omega/2(D-1)} \eta(t). \quad (18)$$

This equation describes an unbiased random walk with a step size varying according to the power law $N_p(t)^\gamma$ with exponent $\gamma = \omega/2(D-1)$. The value of the exponent γ has to be determined either theoretically, or from computer simulations data.

D. Derivation of the first-passage time distribution

Let us consider a Langevin equation describing a continuous-time random walk ξ with a power-law dependence $|\xi|^\gamma$ of the diffusion coefficient,

$$\frac{d\xi(t)}{dt} = D_0 |\xi(t)|^\gamma \eta(t), \quad (19)$$

where D_0 is a numerical factor, the exponent $\gamma \in [0,1)$, and $\eta(t)$ is a normally distributed random variable with zero mean and unit variance. In the particular case

$$D_0 = \frac{\sqrt{2\mu_2}}{1 + \mu_2}, \quad \gamma = \beta/2(D - 1), \quad (20)$$

we recover Eq. (18). The corresponding Fokker-Planck (FP) equation for the time-dependent distribution density $W(t, x)$ of the random variable ξ on the positive real axis $0 \leq x < \infty$ reads

$$\frac{\partial}{\partial t} W = L_{FP} W, \quad \text{with} \quad L_{FP} = D_0^2 \frac{\partial^2}{\partial x^2} x^{2\gamma}. \quad (21)$$

The nonstationary solutions of Eq. (21) can be obtained by the method of separation of variables [20],

$$W(t, x) = e^{-\lambda t} f(x), \quad (22)$$

which leads to the problem

$$D_0^2 \frac{\partial^2}{\partial x^2} x^{2\gamma} f(x) = -\lambda f(x) \quad (23)$$

on $0 \leq x < \infty$, with $\lambda > 0$. The functions $f_{\gamma, \lambda}(x)$ which solve Eq. (23) for the continuous spectrum $-\lambda < 0$ are

$$f_{\gamma, \lambda}(x) = C x^{1/2-2\gamma} J_\nu \left(\frac{\sqrt{\lambda}}{(1-\gamma)D_0} x^{1-\gamma} \right). \quad (24)$$

where J_ν is the Bessel function of the first kind and order $\nu = [2(1-\gamma)]^{-1}$. For $\gamma > 0$ this solution satisfies the boundary

conditions [20]: (a) $x^{2\gamma} f_{\gamma, \lambda}(x) \rightarrow 0$ as $x \rightarrow 0$ (absorbing wall at $x=0$) and (b) the probability current

$$S_{\gamma, \lambda}(x, t) = -D_0^2 e^{-\lambda t} \frac{\partial}{\partial x} f_{\gamma, \lambda}(x) \quad (25)$$

vanishes as $x \rightarrow \infty$ (reflecting wall at $x=\infty$).

Our first aim is to derive the transition probability density $P(x, t | x', t')$ which solves Eq. (21) with the initial condition

$$P(x, t | x', t') = \delta(x - x') \quad (26)$$

and the boundary condition $P(0, t | x', t') = 0$. We recall that $P(x, t | x', t')$ as a function of x' and t' satisfies the backward Kolmogorov equation

$$\frac{\partial}{\partial t'} P = L_{FP}^\dagger P, \quad \text{with} \quad L_{FP}^\dagger = D_0^2 (x')^{2\gamma} \frac{\partial^2}{\partial (x')^2}. \quad (27)$$

The separation of variables ansatz now leads to the problem

$$D_0^2 (x')^{2\gamma} \frac{\partial^2}{\partial (x')^2} f^\dagger(x') = \lambda f^\dagger(x') \quad (28)$$

on $0 \leq x' < \infty$, with $\lambda > 0$, which is solved by

$$f_{\gamma, \lambda}^\dagger(x') = C' (x')^{1/2} J_\nu \left(\frac{\sqrt{\lambda}}{(1-\gamma)D_0} (x')^{1-\gamma} \right). \quad (29)$$

Finally, taking into account the closure equation for the Bessel functions, we arrive at the expression ($t > t'$),

$$\begin{aligned} P_\gamma(x, t | x', t') &= \frac{x^{1/2-2\gamma} (x')^{1/2}}{2(1-\gamma)D_0^2} \int_0^\infty d\lambda J_\nu \left(\frac{\sqrt{\lambda}}{(1-\gamma)D_0} x^{1-\gamma} \right) J_\nu \left(\frac{\sqrt{\lambda}}{(1-\gamma)D_0} (x')^{1-\gamma} \right) e^{-\lambda(t-t')} \\ &= \frac{x^{1/2-2\gamma} (x')^{1/2}}{2(1-\gamma)D_0^2 (t-t')} \exp \left(-\frac{x^{2(1-\gamma)} + (x')^{2(1-\gamma)}}{4(1-\gamma)^2 D_0^2 (t-t')} \right) I_\nu \left(\frac{2(x x')^{1-\gamma}}{4(1-\gamma)^2 D_0^2 (t-t')} \right), \end{aligned} \quad (30)$$

where I_ν is the modified Bessel function of the first kind and order $\nu = [2(1-\gamma)]^{-1}$. It is readily seen that at $\gamma=0$ (then $\nu = 1/2$) and $D_0^2 = 1/2$ one recovers the transition probability density for the ordinary Brownian motion with one absorbing wall at $x=0$.

Now, the density of the first-passage time probability distribution, under the initial conditions $x'=1, t'=0$ appropriate for avalanches, is

$$\begin{aligned} p_\gamma(t) &= -\frac{\partial}{\partial t} \int_0^\infty dx P_\gamma(x, t | 1, 0) \\ &= -\frac{\partial}{\partial t} \frac{1}{2(1-\gamma)D_0^2 t} \int_0^\infty dx x^{1/2-2\gamma} \\ &\quad \times \exp \left(-\frac{x^{2(1-\gamma)} + 1}{4(1-\gamma)^2 D_0^2 t} \right) I_\nu \left(\frac{2x^{1-\gamma}}{4(1-\gamma)^2 D_0^2 t} \right) \end{aligned}$$

$$= \frac{t^{-(1+\nu)}}{\Gamma(\nu) (D_0/\nu)^{2\nu}} \exp \left(-\frac{\nu^2}{D_0^2 t} \right). \quad (31)$$

Hence, we obtain the simple result

$$\tau_t = \frac{3-2\gamma}{2-2\gamma}, \quad (32)$$

which yields the well known exponents $\tau_t = 3/2$ at $\gamma=0$, and $\tau_t = 7/4$ at $\gamma=1/3$; at $\gamma=1/2$ the value $\tau_t = 2$ has been checked numerically.

IV. NUMERICAL RESULTS

A. On the random walk description

It is interesting to note that the proper value of the exponent $D=7/4$ follows from elementary random walk considerations. If one supposes that the leftmost and rightmost un-

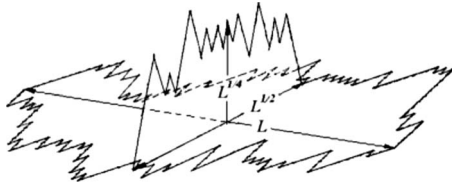


FIG. 2. Interpretation of the fractal dimension $D=1.75$ of the unstable avalanche cluster in terms of simple random walks: $L^D = L \times L^{1/2} \times L^{1/4}$.

stable sites of the avalanche front perform simple random walks, one to the left and the other to the right of the direction of propagation, then the front width will grow with the avalanche length L as $L^{1/2}$. Similarly, take the upper line of an avalanche cross section which describes the height distribution of the unstable sites at a given moment of time. It could also be considered as a positive simple random walk. About the middle of the avalanche the length of this walk is of the order of $L^{1/2}$, hence the maximum height of the unstable sites will scale as $L^{1/4}$. Therefore, the volume of the unstable avalanche cluster is of the order $L^{7/4}$, see Fig. 2 for illustration.

Our computer simulations are done for a directed stochastic sandpile model on the lattice shown in Fig. 1. The transversal direction is labeled by x and in the direction of propagation t (along the diagonal of the squares) the lattice ends up with open boundary conditions. A new avalanche is initiated by adding particles to the top site of the lattice (1,1). When the height at a given site (x,t) equals or exceeds $z_c = 2$ it topples. The toppling rules are more general than the ones used in the earlier theoretical studies [13,14]. Namely, with probability μ_1 only one particle is transferred to the next layer, with equal probability $1/2$ to the right neighbor or to the left one. With probability $\mu_2 = 1 - \mu_1$ two particles are transferred to the nearest neighbors in the next layer; with equal probability $1/3$ the two particles go to the left neighbor, to the right neighbor, or each of the two neighbors in the next layer gets one particle. Nevertheless, as we have shown in Sec. III C, the generated avalanches belong to the same universality class. In order to study the statistical properties of directed avalanches, especially, to analyze their structure from the initial to the final stage of development, simulations for lattice sizes $L=1000$ to $L=15\,000$ were performed, with averaging over 10^3 to 10^9 realizations depending on the random events studied.

The simulation programs and statistical accuracy were tested by data collapse analysis of the integrated avalanche size distribution density, see Eq. (1),

$$P(s) := \int_s^\infty p_s(x) dx.$$

An independent test was provided by the numerical estimation of the exponent τ_s for the avalanche size distribution. The value $\tau_s = 1.432(2)$ obtained for a finite lattice of 3200 time layers and evaluated by linear approximation to the data in the interval of sizes from 200 to 1000, deviates from the

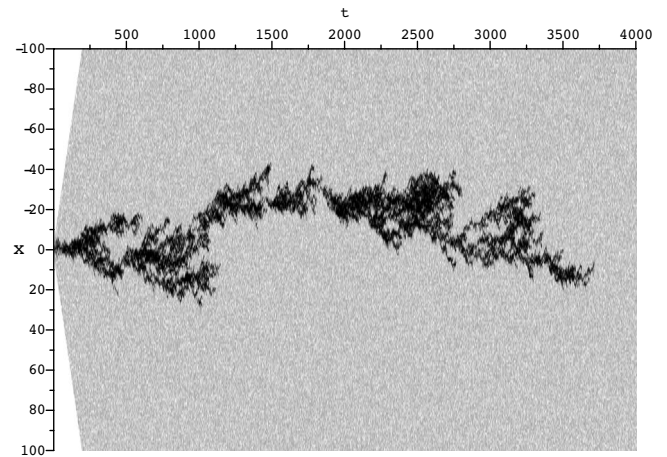


FIG. 3. Trace of a typical avalanche in space (x)-time (t).

exact analytical result $10/7 = 1.428\,57\dots$ for infinite lattices by some 4×10^{-3} .

The real picture of an avalanche evolution happened to be more complicated than the simple random walk description would suggest, as one can see from the trace of a typical avalanche shown in Fig. 3. Obviously, one has to take into account branching and creation of voids, as well as dying out of branches and collapse of voids, processes which may lead to asymmetry in the quantitative description of the different stages of the avalanche development.

Actually, the statistical behavior of the leftmost and rightmost sites of the avalanche front cannot be described as an average displacement of a simple random walk. Indeed, as it is shown in Fig. 4, the front width may grow only by one or two sites at a time step, but from time to time it shrinks down by a large number of sites.

To assess the effect of the above factors on the averaged avalanche characteristics, we have numerically estimated the average values of the front width, the number of unstable sites and the number of toppled particles (momentary size) as a function of time (or the layer position) for a sample of 1000 realizations of avalanches of duration between 8000 and 8080. The latter sample was drawn out of some 2.5×10^7 nonzero avalanches.

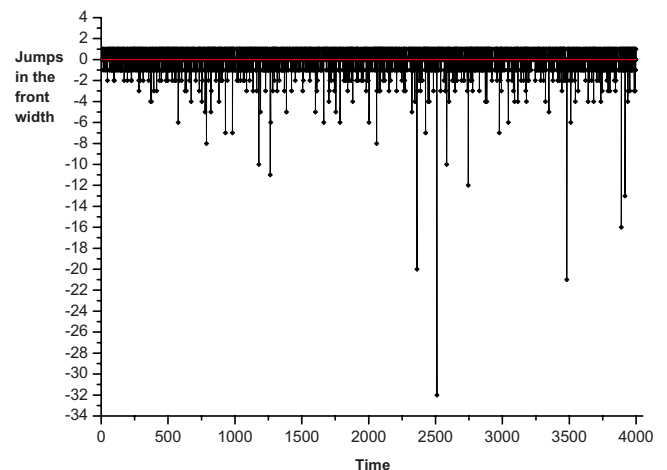


FIG. 4. (Color online) Jumps of the front width at successive moments of time in an avalanche of length 4 028.

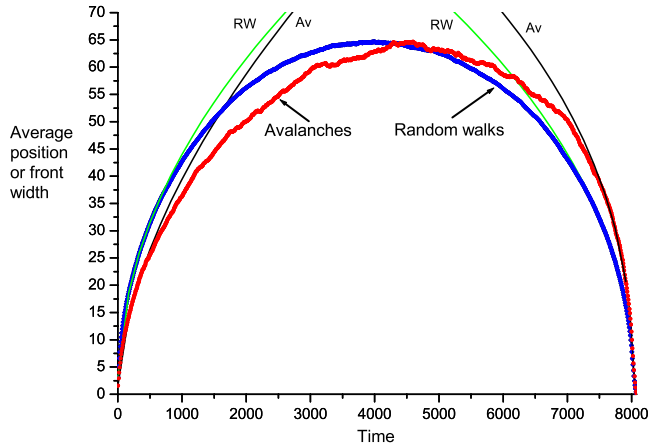


FIG. 5. (Color online) Average front width as a function of the time step for 1000 avalanches of duration between 8000 and 8080 compared with the average position (rescaled by the factor 0.83) of simple random walks of the same length. Power-law fits yield exponent 0.57(1) for the avalanches in the initial stage and 0.41(2) in the final stage. For the random walks the corresponding exponents are 0.48(1) and 0.46(2).

The asymmetry in the time distribution of the average front width is best seen in comparison with the symmetric average displacement of simple random walks, see Fig. 5. The average values were estimated from samples of 1000 realizations of avalanches and 10000 of simple random walks, both of duration between 8000 and 8080. The sample of random walks was drawn out of some 2.3×10^8 nonzero realizations. Clearly, the curves significantly deviate from each other.

Note that the conditional average characteristics of the avalanches, such as the front width, number of unstable sites, number of toppled particles, under the condition that the avalanche must terminate at time T , have to smoothly increase in the growth phase, reach a maximum (or maxima) and then decrease to zero at time $t=T$. Therefore, one can expect a power-law behavior only for small times and for times close to T . An example of such asymptotic power-law behavior is provided by Alcaraz and Rittenberg [18]. They have shown that the conditional average position $\langle x \rangle_{t,T}$ of simple random walks at time $0 < t < T$, under the condition that their first passage time is T , obeys the scaling law $\langle x \rangle_{t,T} = \sqrt{DT}f(t/T)$. By using the Stirling approximation for the factorials, for values $x \ll t \ll T$ and $x^2 \ll T$, one obtains $\langle x \rangle_{t,T} \propto t^{1/2}$. Therefore, in this case one has a simple power-law only as asymptotic behavior. Naturally, for more complicated stochastic processes, which lead in the continuum limit to subdiffusive or superdiffusive behavior, one should expect a different from $1/2$ exponent.

Since we do not pursue an accurate estimation of the scaling exponents, we prefer to use the transparent method of fitting segments of the curves in the growth and terminal stages of the avalanche development with the aid of the nonlinear curve fit program from the Data Analysis and Graphing Software ORIGINPRO 7.5. The intervals to be fitted were chosen of length $0.05T$, where T is the total avalanche duration, so that the left interval is $1 \leq t \leq 0.05T$, and the right

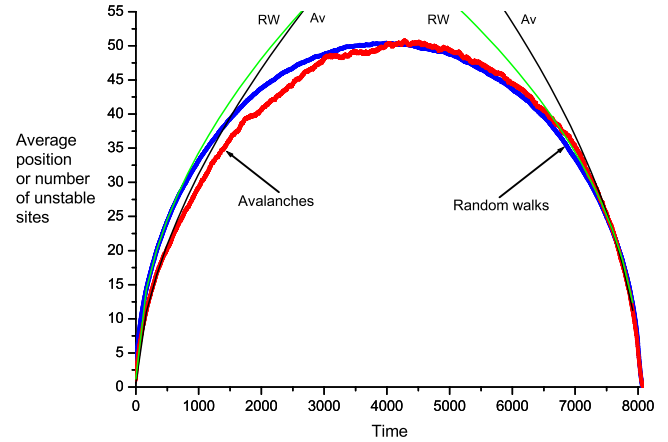


FIG. 6. (Color online) Temporal distribution of the average number of unstable sites for 1000 avalanches of time duration between 8000 and 8080 compared with the average position (rescaled by the factor 0.708) of simple random walks of the same length. Power-law fits yield exponent 0.58(1) for the avalanches in the initial stage and 0.54(1) in the final stage. For the random walks the corresponding exponents are 0.48(1) and 0.46(2).

one is $0.95T \leq t \leq T$. The choice of the value $0.05T$ is based on two criteria: (a) intervals of such a length contain a sufficient number of points even for the smallest $T=1000$ we study, and (b) the values of the avalanche characteristics at $t=0.05T$ and $t=0.95T$ lie between $1/4$ and $1/2$ of their maximum values for all the considered time durations $T=1000, 2000, 4000, 8000$. The second criterion makes possible a sound identification of the interval $1 \leq t \leq 0.05T$ with the initial growth stage and the interval $0.95T \leq t \leq T$ with the final decay stage in the avalanche evolution. The error bars for the exponents given by the fitting program were typically of the order 10^{-3} . However, the exponents evaluated in ensembles of avalanches of (almost) fixed duration, especially at the terminal point (actually an interval of length $0.01T$ in which all the 1000 avalanches terminate), are rather sensitive to the choice of the fitted interval—its length and position. To get more realistic estimates, the values obtained for the interval $[1, 0.05T]$ ($[0.95T, T]$) were compared with those for the slightly shifted $[0.005T, 0.055T]$ ($[0.945T, 0.995T]$) and shortened $[1, 0.045T]$ ($[0.955T, T]$) intervals. As a rule, the error bars for the exponents in the terminal stage are larger due to the stochastic scatter in the exact avalanche durations.

One expects the number of unstable sites at a given moment of time to be proportional to the current width of the avalanche front. Figure 6 presents a comparison between the time distribution of the average number of unstable sites and the average displacement for 10 000 simple random walks, both of length between 8000 and 8080. The asymmetry is less pronounced than in the case of the front width. It is appreciable in the initial and middle stages of the avalanche development, while in the final stage the two curves almost merge. This feature can be explained by supposing that when a branch of a well developed avalanche dies out, only a rather small fraction of the unstable sites is lost. Indeed, the jump size distribution for the number of unstable sites (not shown here) is significantly steeper in the positive direction, but its asymmetry is less pronounced than in the case of the front width.

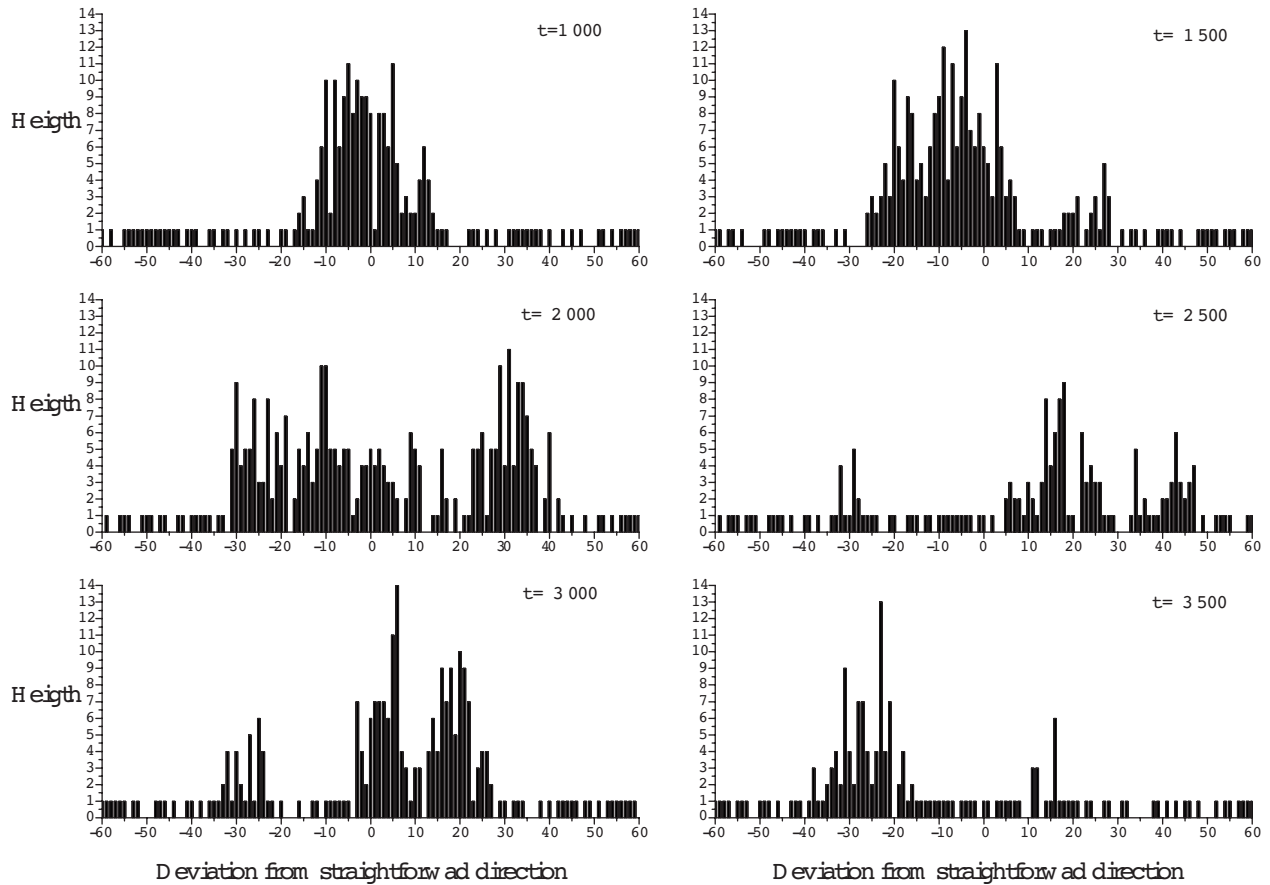


FIG. 7. Profiles of the front of a long avalanche, which reaches the open boundary of a lattice of size 15 000, taken at intervals of time $\Delta t=500$.

We note also that the height distribution of the unstable sites at a given moment of time cannot be described by a simple random walk too. The profiles shown in Fig. 7 exemplify that during some stages of evolution the height distribution represents a sequence of random walks, separated by intervals of stable sites. It is not clear whether the number of these separate walks remains bounded when the length of the avalanche increases infinitely.

Although some of the above discussed features pertain to individual realizations of avalanches only, and are smeared out in the statistical description, they still affect the probability distributions. For example, the exponents of the power-law conditional distributions for the front width and the number of unstable sites in finite-size avalanches differ in the growth and decay stages. In spite of the apparent asymmetry in the avalanche development, it seems insufficient to affect the fractal dimension D of the total avalanche cluster.

A new and quite interesting result yields the comparison of the time-dependence of the average number of toppled grains and the conditional average position of random walks with step size varying according to the theory [14]. To this end we have evaluated numerically the corresponding distributions, as a function of time, under the condition that the length of both the avalanches and random walks belongs to the interval $L \in (8000, 8080)$, see Fig. 8. Evidently, the curves for the avalanches and the random walks remain fairly close to each other during the entire time evolution.

B. Finite-size scaling analysis

Here we report results on the data collapse, under suitable finite-size scaling transformations, for the time-dependent front width, Fig. 9, number of unstable sites, Fig. 10, and number of toppling particles, Fig. 11, evaluated in restricted

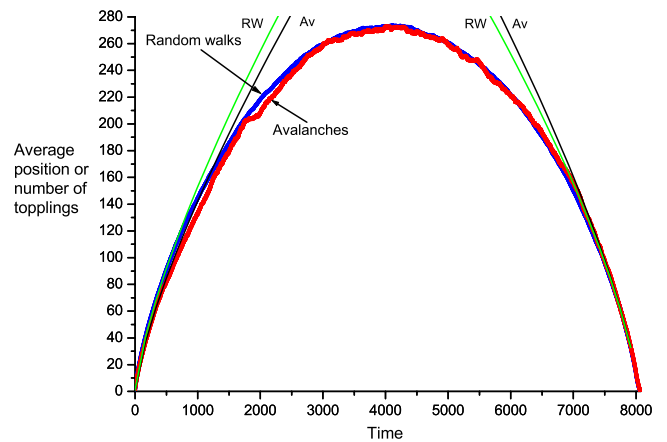


FIG. 8. (Color online) Average number of topplings in a layer for avalanches of length between 8000 and 8080 compared with the average position (rescaled by a factor 0.83) of random walks of the same length with step size varying as the cubic root of the current position.

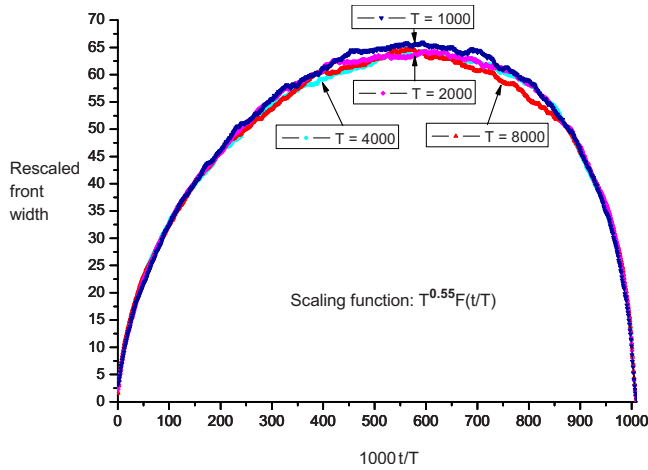


FIG. 9. (Color online) Finite-size data collapse for the temporal distribution of the avalanche front width for avalanches with duration $T=1000, 2000, 4000,$ and 8000 . The scaling function is $T^{0.55}F(t/T)$.

ensembles of avalanche duration in the intervals $[T, 1.01T]$, where $T=1000, 2000, 4000,$ and 8000 .

In all three cases the data collapse is rather good in the wings of the conditional distributions which are, presumably, described by power laws. This collapse is an important evidence for the existence of finite-size scaling laws describing the entire avalanche evolution. The largest deviations are observed in the region about the maximum value, where we expect large fluctuations due to branching and formation of holes in the process of evolution.

The most asymmetric distribution is the one of the avalanche front width, see Fig. 9. This can be attributed to the diffusive growth of almost compact front in the early growth stage, and the abrupt extinction of side branches in the final decay stage. This scenario will be further analyzed in Sec. V.

The finite-size effects on our estimates of the scaling exponents for the front width growth and decay are shown in Fig. 12. The trend downward with the increase of T is probably due to corrections to scaling. However, the points are

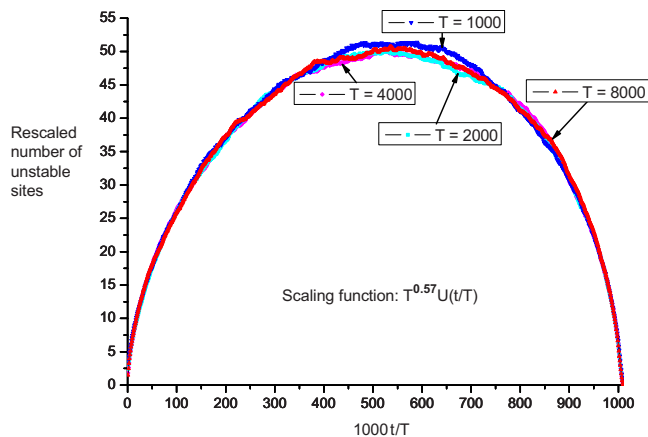


FIG. 10. (Color online) Finite-size data collapse for the temporal distribution of the number of unstable sites for avalanches with duration $T=1000, 2000, 4000,$ and 8000 . The scaling function is $T^{0.57}U(t/T)$.

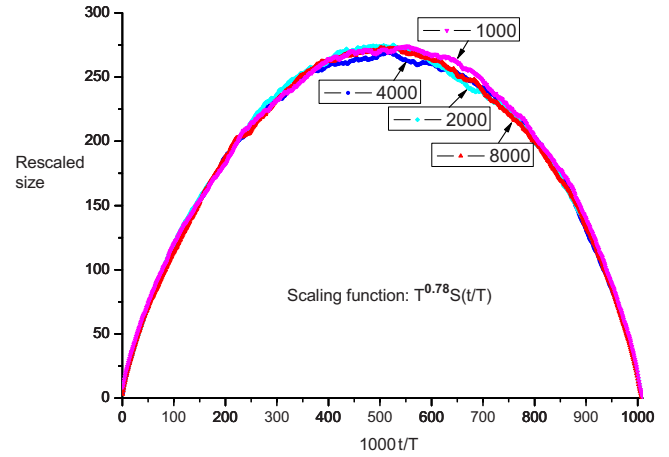


FIG. 11. (Color online) Finite-size data collapse for the temporal distribution of the number of topplings for avalanches with duration $T=1000, 2000, 4000,$ and 8000 . The scaling function is $T^{0.78}S(t/T)$.

two few for making reliable estimates of the limit $T \rightarrow \infty$.

The temporal distribution of the number of unstable sites, shown in Fig. 10, shows less asymmetry. Accordingly, the evaluated exponents in the growth and decay stages are rather close to each other and, unexpectedly, a crossover from larger exponents at the terminal point to larger exponents at the initial point takes place between $T=2000$ and $T=4000$, see Fig. 13.

In the case of the temporal distribution of the number of topplings, the growth and decay exponents (not shown) are very close to each other, their error bars overlap, and the slight trend upward tends to the value of 0.75 with the increase of T . Obviously, data for still longer avalanches are necessary for evaluation of the above exponents in the limit $T \rightarrow \infty$.

V. DISCUSSION AND SUMMARY

It seems that the existing theoretical approaches, leading to continuous stochastic equations, yield the exact values of the exponents characterizing avalanches in directed stochas-

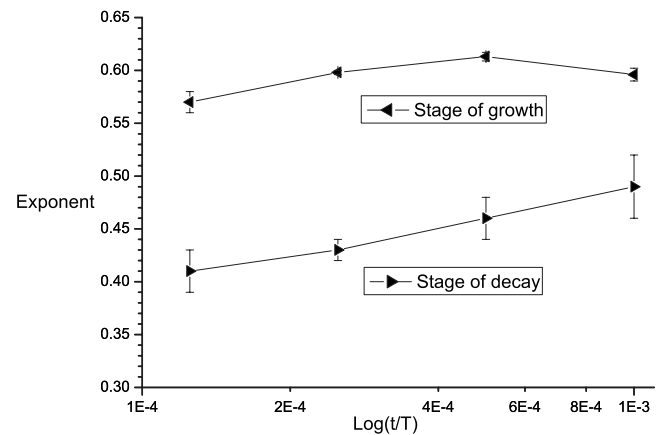


FIG. 12. Finite-size dependence of the exponents for the avalanche front width.

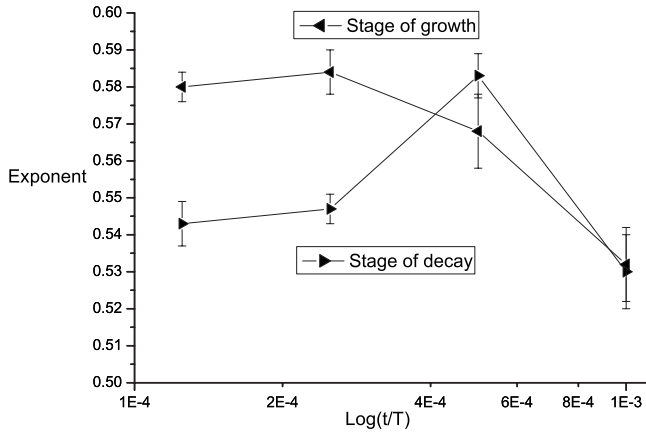


FIG. 13. Finite-size dependence of the exponents for the number of unstable sites.

tic sandpiles. However, we point out that the derivation of these exponents is not rigorous.

In the theory of [13] the nonlinearity in the stochastic differential Eq. (5), due to the presence of the threshold step function, is removed without analysis of its relevance. Thus, the derivation of the scaling exponents is based on the linear EW equation which models the stochastic kinetics of a growing surface [19]. It describes surface roughening, caused by the fluctuations in the flux of deposited atoms, which obeys a dynamic scaling law. In the case under consideration, the solution of the EW equation in the interval $|x| \leq L$ displays root mean square fluctuations $w_L(t)$ of the number of grains $n(x, t)$ transferred to site (x, t) which obey the finite-size scaling law

$$w_L(t) \equiv [\langle n^2(x, t) \rangle - \langle n(x, t) \rangle^2]^{1/2} \simeq L^\alpha W(t/L^\zeta). \quad (33)$$

Here $\langle \cdot \rangle$ denotes averaging over the noise, α is the roughening exponent and ζ the dynamic exponent; the scaling function W has the asymptotic behavior $W(u) \sim u^\beta$ as $u \rightarrow 0$, β being the growth exponent, and $W(u) \rightarrow \text{const}$ as $u \rightarrow \infty$. In the one-dimensional EW universality class with uncorrelated noise, the values of the exponents are $\alpha = 1/2$, $\beta = 1/4$, and $\zeta = \alpha/\beta = 2$. The dynamic exponent ζ describes how the time t_x of crossover from growth to saturation scales with the system size, $t_x \sim L^\zeta$.

The crucial point in the theory of [13] is the identification of the scaling law for the maximum number of topplings, n_c , with Eq. (33) taken at $L \propto x_c$ and $t_x \propto t_c$, where x_c and t_c are the characteristic width and length of the directed avalanches, respectively. Thus one obtains $n_c \sim w_{x_c}(t_c) \sim x_c^{1/2}$ and $x_c \sim t_c^{1/2}$. This result readily follows from simple arguments. For times $t \geq t_x \sim L^2$, the profile of $n(x, t)$, considered on a space interval of fixed length L , flattens out, $n(x, t) \approx n_L(t)$, and the diffusion term in the linear EW Eq. (7) becomes negligible. What remains is a Langevin equation for the variable $n_L(t)$ which provides a continuous-time description of the simple random walk performed by $n_L(t)$. Hence, the scaling $n_c \sim x_c^{1/2}$ follows after identifying n_c with the root mean fluctuations of $n_L(t)$ and the interval L with x_c .

In the theory of [14] the value 1/2 of the exponent in the scaling relationship $N_u(t) \sim t^{1/2}$, which we denote by ω , can be justified on the following grounds.

(a) Let the front $F(t)$ of an avalanche at time t be defined as the set of sites between the leftmost and rightmost unstable (at that moment of time) sites, and the front width $u(t)$ be the distance between these sites. The average width $\langle u(t) \rangle$ of the avalanche front is supposed to grow with time t as the average distance from the origin of a simple random walk, i.e., for sufficiently large times it is proportional to $t^{1/2}$.

(b) The core of the avalanche at any given time is relatively hole free, so that asymptotically the number of unstable sites $N_u(t) \sim t^{1/2}$, i.e., $\omega = 1/2$. In such a case, taking into account that $D = 7/4$, one obtains the result [14]

$$\gamma = \frac{\omega}{2(D-1)} = \frac{1}{3}. \quad (34)$$

We think that the above arguments miss the following point: the evolution of individual long avalanches, excluding relatively short initial and final stages, has a somewhat self-similar, pulsating nature. Actually, a long period of propagation is characterized by interchanging processes of growth in width, height and flow of particles with the processes of decay, when the avalanche parameters decrease to rather small values. At such “bottlenecks” the evolution is no longer governed by a dense front of sites with large number of topplings, and the appearance of holes and separation of branches becomes probable, see Figs. 3 and 7.

We can suggest another plausible scenario for the avalanche evolution, based on the following conjecture: the average number of unstable sites $N_u(t)$ grows with time t with exponent $\omega < 1/2$. Such a behavior may have at least two different origins.

(i) The strong asymmetry between the jumps up (just by one lattice spacing) and down (occasionally, by a large number of lattice spacings), which is due to dying out of some of the branches of the avalanche, may change the exponent ω in the scaling relationship $N_u(t) \sim t^\omega$, most probably to a lower value. The decrease in ω , however, leads to a decrease in the diffusion exponent γ , see Eq. (34).

(ii) We observe that contrary to the arguments of [14], creation of “holes” (regions of stable sites) is quite probable, see Fig. 7 where profiles of the front of a long avalanche, taken at different moments of time, are shown. As the avalanche advances, the holes in its front either collapse or lead to the creation of “branches”—offsprings of the avalanche “backbone” which propagate and die out on their own.

To evaluate the effect of the holes formation on the avalanche propagation, we have defined width $w_\Delta(t)$ of the backbone (thickest branch) of an avalanche at a moment of time t as follows: the front $F(t)$ of an avalanche at time t , is split into subsets $\{S_\Delta^i\} \subset F(t)$ of “ Δ -dense” unstable sites, separated by gaps of stable sites, so that: (a) the distance between any pair of closest toppling sites in every subset $S_\Delta^i(t)$ is less than $\Delta > 1$ and (b) the distance (gap) between any two subsets $S_\Delta^i(t)$ and $S_\Delta^j(t)$ is equal to or larger than Δ . Then, the largest value $w_\Delta(t) = \max_i \text{diam} S_\Delta^i(t)$ is registered and averaged over a sample of long enough avalanches. The

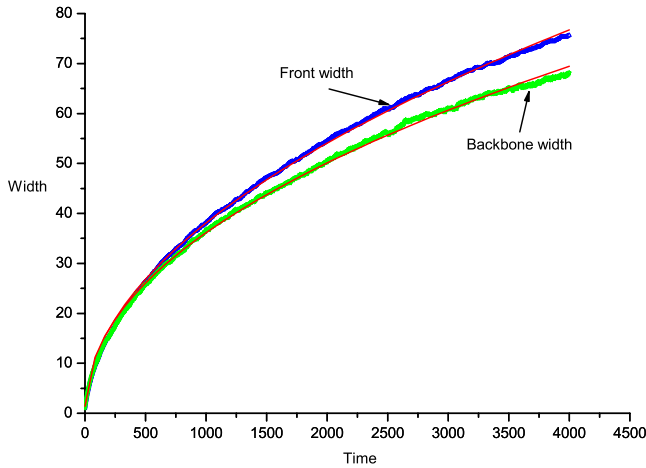


FIG. 14. (Color online) Average front width and backbone width as a function of time in the growth stage of 1000 avalanches lasting longer than 12000. The best power-law fits are shown by thin lines.

averaged over 1000 realizations of avalanches longer than 12 000 width of the backbone $\langle w_{\Delta}(t) \rangle$ is shown in Fig. 14 for $\Delta=10$ at times $t=1, 2, \dots, 4500$. For comparison, the time behavior of the average front width $\langle u(t) \rangle = \langle \text{diam} U(t) \rangle$ is shown as well. Obviously, while $\langle u(t) \rangle \sim t^{1/2}$ with fairly good accuracy, the width of the backbone scales as $\langle w_{\Delta}(t) \rangle \sim t^{\omega(\Delta)}$ with $\omega(10) \approx 0.47$ appreciably less than $1/2$.

Finally, one can conjecture that the avalanche lifetime T equals the lifetime of its backbone. In such a case one may argue that the stochastic time behavior of growing avalanches is governed by Eq. (18) with ω somewhat smaller than $1/2$. Of course, this hypothesis can be pursued further provided $\omega(\Delta)$ saturates at some value ω^* as Δ grows, but remains much less than $\langle u(t) \rangle$. However, such a study is out of the scope of the present work. We just mention that a decrease in ω below $1/2$ will cause a decrease in the exponent of the diffusion coefficient γ below $1/3$, which, taking for granted $D=7/4$, will lead to $\tau_i < D=7/4$, see Eq. (32). Such a shift would be in the direction opposite to the one suggested by the most recent computer simulation results [18].

The relevance of Abelian symmetry and stochasticity in directed sandpiles has been discussed in [21]. There a special exponent α_{sc} has been introduced for the time dependence of the trace of avalanche boundary sites (called scars). This exponent is related by the equality $\alpha_{\text{sc}} = D_w$ to the avalanche width exponent D_w . It is then argued that for Abelian deterministic models $D_w = 1/2$ by mapping avalanche boundaries onto simple random walks, and for the Abelian stochastic models the same value $D_w = 1/2$ holds due to the lack of correlations in the unstable patterns. In our study we question the assumption of compactness of avalanches and go deeper than the avalanche boundaries by introducing the notion of Δ -dense avalanche backbone. We can conclude that the relationship between the spatial structure of directed avalanches and their statistical characteristics needs further investigations.

It would be interesting to carry out a similar study for an Abelian model with a tunable degree of anisotropy which continuously interpolates between the isotropic and directed

sandpiles. Then one could check the hypothesis that the universality class remains the same for all systems with nonvanishing degree of anisotropy. In the case of the Oslo model such program has been fulfilled in [22].

Finally, we summarize our main contributions.

(1) We have extended the theory of Kloster-Maslov-Tang [14] in two important aspects:

(a) The existing theory was based on the simplest case when unstable sites may transfer only an even number of particles to the next layer. This simplification makes possible an easy identification of the active sites (those which change the flux by one) as the sites which receive an odd number of particles from the previous layer, i.e., on the average such are $1/2$ of all unstable sites in the layer. Our extension introduces a new probabilistic element by allowing the unstable sites to transfer both even and odd number of particles with probabilities [Eqs. (9) and (10)]. So, it is by no means obvious that the probability of two-particles toppling μ_2 will enter only into the coefficient of the diffusion term and will not change its exponent, see Eq. (18).

(b) It is shown that the conjectured in Ref. [14] simple diffusionlike growth with time of the number of unstable sites, $N_u(t) \propto t^{1/2}$, can be replaced by a more general power law $N_u(t) \propto t^{\omega}$. Such an extension is necessary because our simulation data show that, contrary to the arguments in [14], the avalanche front is not compact, see Figs. 3 and 7, and its boundaries do not perform simple random walks, as is evident from Figs. 3 and 4. The deviation from the simple random walk picture of the front width persist in the data averaged over the ensemble of 1000 avalanches of almost fixed duration, as shown in Fig. 5.

(2) A new result, and of special interest in its own right, is the solution of the Fokker-Planck equation with a diffusion coefficient in the form of a singular power-law function of the spatial coordinate. It turned out possible to integrate it completely and, rather surprisingly, to obtain a simple expression for the density of the probability distribution for the lifetimes of unbiased random walks with a step size varying with the current position $\xi(t)$ as $|\xi(t)|^{\gamma}$, see Sec. III D.

(3) Our simulations and their analysis did not aim at the precise evaluation of scaling exponents. Our main goal was to advance a novel approach in the study of avalanches—evaluation of their properties in an ensemble of avalanches with almost fixed (within tolerance of 1%) time duration, less than the lattice size in the temporal direction. This made possible the study of statistical properties of similar avalanches during their complete evolution. In particular, we have quantitatively evaluated the asymmetry between the time dependence of the front width and the number of unstable sites in the initial and final stages of development in an ensemble of 1000 avalanches with lifetimes in the interval between 8000 and 8080. Up to our knowledge, we have shown for the first time that the terminal stage of the avalanche evolution can be described by power-law exponents different from those for the growth stage.

(4) By using the method of data collapse we have established the existence of finite-size scaling laws describing the entire evolution of avalanches. It was found that the whole

temporal profile of the number of topplings is very well described by the theory of Kloster, Maslov, and Tang as a random walk with step size varying as the cubic root of the displacement.

(5) To quantitatively assess the effect of possible deviations from compactness of avalanches on their lifetime distribution, we introduced the notion of “ Δ -dense” avalanche backbone. Quite surprisingly, we have found that for $\Delta=10$ the backbone, averaged over 1000 avalanches lasting for

more than 12 000 time steps, grows with time subdiffusively with exponent about 0.47.

ACKNOWLEDGMENTS

I am grateful to V. B. Priezzhev for suggesting the problem and his constant attention to the work. I thank also J. G. Brankov for helpful comments and discussions. This work was supported by Grant No. 248/23.04.08 of the Representative Plenipotentiary of Bulgaria at JINR.

-
- [1] P. Bak, C. Tang, and K. Wiesenfeld, *Phys. Rev. Lett.* **59**, 381 (1987).
- [2] T. Hwa and M. Kardar, *Phys. Rev. Lett.* **62**, 1813 (1989).
- [3] A. Diaz-Guilera, *Phys. Rev. A* **45**, 8551 (1992).
- [4] D. Dhar, *Phys. Rev. Lett.* **64**, 1613 (1990).
- [5] V. B. Priezzhev, D. V. Kitarev, and E. V. Ivashkevich, *Phys. Rev. Lett.* **76**, 2093 (1996).
- [6] E. V. Ivashkevich and V. B. Priezzhev, *Physica A* **254**, 97 (1998).
- [7] D. Dhar, *Physica A* **263**, 4 (1999).
- [8] D. Dhar and R. Ramaswamy, *Phys. Rev. Lett.* **63**, 1659 (1989).
- [9] S. S. Manna, *J. Phys. A* **24**, L363 (1991).
- [10] A. Vespignani, S. Zapperi, and L. Pietronero, *Phys. Rev. E* **51**, 1711 (1995).
- [11] J. Hasty and K. Wiesenfeld, *Phys. Rev. Lett.* **81**, 1722 (1998).
- [12] A. Chessa, H. E. Stanley, A. Vespignani, and S. Zapperi, *Phys. Rev. E* **59**, R12 (1999).
- [13] M. Paczuski and K. E. Bassler, *Phys. Rev. E* **62**, 5347 (2000).
- [14] M. Kloster, S. Maslov, and C. Tang, *Phys. Rev. E* **63**, 026111 (2001).
- [15] M. Stapleton and K. Christensen, *J. Phys. A* **39**, 9107 (2006).
- [16] A. Vazquez, e-print [arXiv:cond-mat/0003420](https://arxiv.org/abs/cond-mat/0003420).
- [17] R. Pastor-Satorras and A. Vespignani, *J. Phys. A* **33**, L33 (2000); *Phys. Rev. E* **62**, 6195 (2000).
- [18] F. C. Alcaraz and V. Rittenberg, *Phys. Rev. E* **78**, 041126 (2008).
- [19] S. F. Edwards and D. R. Wilkinson, *Proc. R. Soc. London, Ser. A* **381**, 17 (1982).
- [20] H. Risken, *The Fokker-Planck Equation: Methods of Solution and Applications* (Springer-Verlag, Berlin, 1989).
- [21] H.-H. Jo and M. Ha, *Phys. Rev. Lett.* **101**, 218001 (2008).
- [22] G. Pruessner and H. J. Jensen, *Phys. Rev. Lett.* **91**, 244303 (2003).